ChemComm

Accepted Manuscript

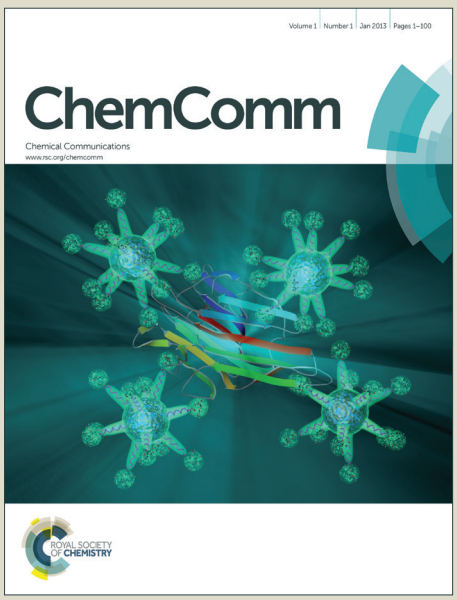

ROYAL SOCIETY OF CHEMISTRY

www.rsc.org/chemcomm

ChemComm

RSCPublishing

COMMUNICATION

Highly Efficient Molecular Nickel Catalysts for Electrochemical Hydrogen Production from Neutral Water

Cite this: DOI: 10.1039/x0xx00000x

Peili Zhang,[a] Mei Wang,*[a] Yong Yang,[a] Dehua Zheng,[a] Kai Han[a] and Licheng Sun[a,b]

Received 00th January 2012,
Accepted 00th January 2012

DOI: 10.1039/x0xx00000x

www.rsc.org/

A series of nickel complexes containing N_5-pentadentate ligands with different amine-to-pyridine ratios were studied for electrochemical H_2 production in neutral water and the one with a diamine-tripyridine ligand displays a TON up to 308,000 over 60-h electrolysis at −1.25 V vs. SHE, with a Faradaic efficiency of ~91%.

Electrolysis of water to hydrogen is a practical and promising way to store the surplus electric power, generated by renewable energy sources such as sun light, wind, tides, etc. and distributed unevenly in seasons and districts. Development of electrocatalysts that are made from earth-abundant elements and work in fully aqueous solutions with high activity, low overpotential, and good durability remains one of the crucial issues to be solved for the realization of an energy-efficient and cost-effective transformation of electric power to hydrogen.[1] In recent years, numerous molecular catalysts based on earth abundant elements were reported to be efficient for electrochemical H_2 generation, but most of them work for reduction of protons from organic or inorganic acids in organic solutions or the mixture of organic solvent and water.[2,3] To date, non-noble metal-based molecular catalysts that function in fully aqueous solutions,[4,5] especially in neutral aqueous solutions, are quite few. The representative ones are nickel macrocycles,[6] cobalt macrocycles,[7] $[(PY5Me_2)MoO]^{2+}$ ($PY5Me_2$ = 2,6-bis(1,1-bis(2-pyridyl)ethyl)pyridine),[8] $[(PY5Me_2)Co(H_2O)]^{2+}$,[9,10] (DPA-Bpy)$Co(H_2O)]^{3+}$ (DPA-Bpy = *N*,*N*-bis(2-pyridinylmethyl)-2,2'-bipyridine-6-methanamine),[11] $[(bztpen)Co(H_2O)]^{2+}$ (bztpen = *N*-benzyl-*N*,*N*',*N*'-tris(2-pyridylmethyl)ethylenediamine),[12] and a cobalt catalyst bearing a multihydroxy-functionalized tetraphosphine ligand.[13]

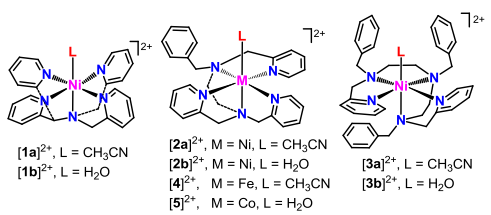

Fig. 1 Structures of nickel, iron and cobalt N_5-pentadentate complexes used as molecular electrocatalysts in the present work

Although nickel is one of the two metals used by nature to build the active site of [NiFe]-hydrogenases and also the most active non-precious metal for electrochemical proton reduction to hydrogen,[14] nickel-based molecular electrocatalysts so far reported for H_2 production are limited, including nickel N_4-macrocyclic complexes,[6] diimine-dioxime complexes,[15] pyridinediimine complex,[16] dithiolene complex,[5] thiolate complexes,[17] and nickel complexes with amine-containing diphosphine ligands.[18] Among these nickel catalysts, only two of them, namely $[Ni(cyclam)]^{2+}$ (cyclam = 1,4,8,11-tetraazacyclotetradecane) and $[Ni(biscyclam)]^{2+}$ (biscyclam = 6,6'-bi-1,4,8,11-tetraazacyclotetradecane), were reported to be catalytically active for electrochemical hydrogen production in neutral aqueous solutions, with turnover numbers (TONs) up to 100 at −1.26 V vs. standard hydrogen electrode (SHE).[6] Here we describe the preparation and the molecular structures of a series of nickel complexes with N_5-pentadentate ligand scaffolds (Fig. 1), $[(Am1Py4)NiL](BF_4)_2$ (**1a**, L = CH_3CN; **1b**, H_2O; Am1Py4 = 1,1-di(2-pyridinyl)-*N*,*N*-bis(2-pyridinylmethyl)methanamine), $[(Am2Py3)NiL](BF_4)_2$ (**2a** and **2b**, Am2Py3 = bztpen), and $[(Am3Py2)NiL](BF_4)_2$ (**3a** and **3b**, Am3Py2 = *N*,*N*'-dibenzyl-*N*-(2-(benzyl(2-pyridinylmethyl)amino)ethyl)-*N*'-(2-pyridinylmethyl)-ethane-1,2-diamine). Studies on the cyclic voltammograms (CVs) and the catalytic behaviours of **1**–**3** showed that their electrochemical properties and catalytic activities are considerably influenced by the amine-to-pyridine ratio in N_5-pentadentate ligands. The H_2-evolving activities are up to 440, 1650, and 85 mol H_2 (mol cat)$^{-1}$ h^{-1} cm^{-2} for **1b**, **2b**, and **3b**, respectively, for 60-h electrolysis experiments in neutral aqueous solutions at an applied potential of −1.25 V (all potentials given in this paper are versus SHE).

Nickel complexes **1a** and **1b** were prepared as amaranthine crystalline solids in 70–81% yields from the reaction of $Ni(BF_4)_2$ $6H_2O$ with Am1Py4 at room temperature in acetonitrile and water, respectively.[19] Similarly, homologous nickel complexes, **2a**, **2b**, **3a**, and **3b** (Figs. S1–S7), were prepared in good yields with essentially identical protocols using corresponding N_5-pentadentate ligands, respectively, in acetonitrile or water. Analogous iron and cobalt complexes, $[(Am2Py3)Fe(NCCH_3)](BF_4)_2$ (**4**) and $[(Am2Py3)Co(H_2O)](BF_4)_2$(**5**) were prepared as reference complexes according to the literature procedures.[12,20]

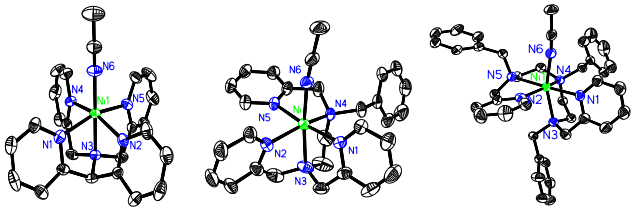

Fig. 2 Structures of cations $[\mathbf{1a}]^{2+}$, $[\mathbf{2a}]^{2+}$, and $[\mathbf{3a}]^{2+}$ with thermal ellipsoids shown at 30% probability; Counterions, solvent molecules and hydrogen atoms are omitted for clarity.

Among the nickel complexes obtained, molecular structures of **1a**, **2a**, **2b**, and **3a** were determined by crystallographic analyses (Figs. 2 and S8, Tables S1–S3). Crystal structures of **1a**–**3a** and **2b** show that the nickel centres in these complexes reside in a distorted octahedral geometry coordinated with a N_5-pentadentate ligand and an acetonitrile or a water molecule bound at an apex, which is opposite to an amine-N atom. The dissociation of the labile ligand, an acetonitrile or a water molecule at apex position, will provide an open site for the coordination of protons to the nickel core.

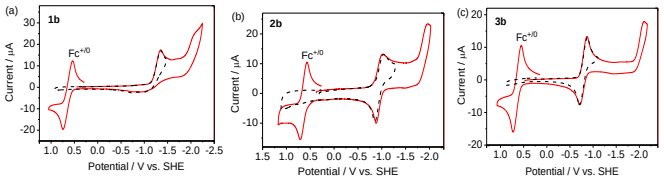

Fig. 3 Cyclic voltammograms of **1b**, **2b** and **3b** in 0.1 M nBu$_4$NPF$_6$/THF with (red solid line) and without (black dashed line) the internal reference (E(Fc$^{+/0}$) = 0.64 V vs. SHE), scan rate 100 mV s^{-1}.

To estimate the influence of amine-to-pyridine ratio in a N_5-pentadentate ligand on the electrochemical property of nickel complexes, the CVs of **1b**–**3b** were studied in Ar-purged THF solutions using a glassy carbon electrode as working electrode (Fig. 3). Raman spectroscopic studies and X-ray diffraction analyses of the crystals that were obtained from the dissolution and recrystallization of **2a** and **2b** in THF, respectively, demonstrate that the apical CH_3CN and H_2O ligands in **2a** and **2b** cannot be substituted by the molecule of solvent, THF (Figs. S9, S10 and S11). Complex **1b** displays an irreversible reduction event at E_{pc} = −1.35 V for the Ni^{II}/Ni^{I} couple, while **2b** and **3b** each exhibit a reversible reduction event at $E_{1/2}$ = −0.94 and −0.79 V. The second reduction peaks of **1b**–**3b** are all irreversible and appear at −2.06, −1.95, and −2.10 V, respectively. The results indicate that the reduction potentials of nickel complexes with a N_5-pentadentate scaffold can be tuned by adjusting the ratio of amine-N to pyridine-N atoms in ligands. It is noticeable that increase of the amine-to-pyridine ratio from 1:4 to 2:3 and then to 3:2 in the ligands of **1b**, **2b**, and **3b** caused the shifts of the first reduction peak for the Ni^{II}/Ni^{I} couple to positive direction by 320 and 480 mV (Table S4). In the same time, the reversibility of the first reduction potentials of N_5-coordinated nickel complexes apparently improved. Similar to **1b**–**3b**, complexes **1a**–**3a** bearing a coordinated apical acetonitrile molecule each display a reduction peak for the Ni^{II}/Ni^{I} couple, at E_{pc}= −1.33, −1.12, and −0.85 V, respectively, which is irreversible in the CV of **1a** and reversible in the CVs of **2a** and **3a** in THF (Fig. S12). The assignment of the first reduction wave to the nickel-centred reduction process is supported by the facts that: (i) the free ligands are all electrochemically silent in the potential scan range of +0.9 to −2.0 V and (ii) the analogous iron complex **4** containing the same ligand as that in **2a** and **2b** is silent in the scan range of −0.7 to −1.3 V in its CV (Fig. S13). The second reduction peaks of **1a**, **2a**, and **3a** are all irreversible, appearing in the range of −2.07 to −1.89 V. A similar shift trend of reduction potentials as that displayed by the series of **1b**, **2b**, and **3b** is observed in the CVs of **1a**, **2a**, and **3a**, with the amine-to-pyridine ratio increasing from 1:4 to 3:2 in the ligand. The separation of two reduction peaks ($\Delta E(E_{pc1} - E_{pc2})$) of these nickel complexes is considerably influenced by the amine-to-pyridine ratio of N_5-pentadentate ligand.

The electrochemical properties of **1b**–**3b** in 1.0 M phosphate buffer at pH 7.0 were investigated under Ar with a controlled growth mercury drop electrode as working electrode (Table S5). The glassy carbon electrode is not suitable for evaluation of the activity of nickel catalysts in neutral aqueous solutions as the background starts rising at about −1.2 V that overlaps the catalytic current (Fig. S14). Complex **2b** exhibits two reduction peaks at −0.98 and −1.05 V prior to the sharp rise in current at −1.12 V (Fig. 4b) and **3b** displays two reduction peaks at −0.69 and −1.16 V before the strong peak arising at −1.22 V (Fig. 4c), while **1b** shows only a strong peak arising at −1.10 V (Fig. 4a). We assume that the reduction peaks of **1b** are overlapped with the broad bottom of catalytic peak. The sharp currents with onset potentials at −1.10 V and −1.13 V for **1b** and **2b**, respectively, are ascribed to the catalytic process for H_2 generation in view of evolution of bubbles from the electrode surface at these potentials. The H_2 evolved was detected by GC analysis. The control experiments show that under identical CV conditions Ni(BF$_4$)$_2$ is electrochemically silent up to −1.4 V in phosphate buffer at pH 7 (Fig. 4b) and the reduction peaks displayed by free ligands, Am1Py4 and Am2Py3, are more negative than the potentials of catalytic peaks exhibited by the corresponding nickel complexes. A comparison of CVs of Fe^{II} (**4**), Co^{II} (**5**),[12] and Ni^{II} (**2b**) complexes containing the same ligand, Am2Py3, in neutral phosphate buffer solutions (Fig. 4d) clearly shows that Co^{II} and Ni^{II} complexes of Am2Py3 display much lower overpotentials and higher catalytic activities than the analogous Fe^{II} complex for electrochemical H_2 evolution from neutral water. The first reduction peak at −1.22 V for the cobalt complex in Fig. 4d is not only corresponding to the Co^{II}/Co^{I} reduction, but also ascribed to a metal-centred catalytic process for the H_2 generation.[12] These results indicate that (i) the nickel complexes containing a N_5-pentadentate ligand are responsible for catalytic process, rather than the simple nickel ion and the free ligand; (ii) the metal in the complex plays an important role in the electrocatalytic H_2 generation. Noticeably, the sharp current appearing in the CV of corresponding complex **3b** is very close to the reduction peak of free ligand Am3Py2. In this context, the catalytic H_2 generation and the ligand-based redox process of **3b** may take place at the same time.

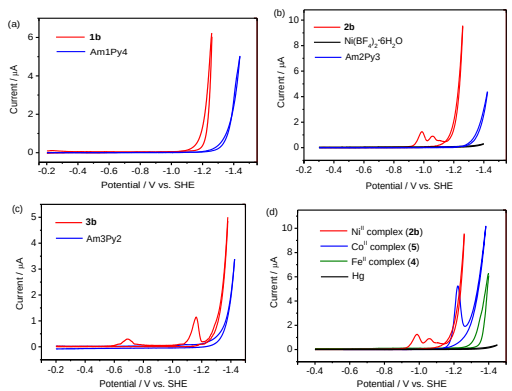

Fig. 4 Cyclic voltammograms of (a) **1b** and Am1Py4; (b) **2b**, Am2Py3, and Ni(BF$_4$)$_2$; (c) **3b** and Am3Py2; (d) Ni^{II} (**2b**), Fe^{II} (**4**), and Co^{II} (**5**) complexes of Am2Py3 ligand; 15 μM in 1.0 M phosphate buffer at pH 7 with a controlled growth mercury drop electrode in a scan rate of 100 mV s^{-1}.

Considering the CVs of **1b**, **2b**, and **3b** in aqueous solutions, **2b** was chosen as an example for the further electrochemical studies. The currents of the reduction peaks of **2b** at −0.98 and −1.05 V enhance linearly with increase of catalyst concentration (Fig. S15). The plots of peak current versus scan rate (Figs. S16, S17a and S18a) for the reduction peaks of **2b** at −0.98 and −1.05 V show that at high scan rates the data deviate from the fitting linear lines with a parabolic trend, while the peak currents exhibit better linear relationship with the root of scan rate (Figs. S17b and S18b). Additionally, the plots of log(*i*) versus log(*v*) for the two reduction peaks display slopes of 0.53 and 0.68 (Figs. S17c and S18c), respectively. It is known that for a typical molecular diffusion-controlled process, the value of slope is 0.5, while for the species confined to the electrode surface, the value of slope is 1.0.[21] If one closely observe the plots of log(*i*) versus log(*v*) in Figs. S16c and S17c, one can find that the slopes of log(*i*) versus log(*v*) obtained in scan rates slower than 200 mV s^{-1} are somewhat different from those obtained in scan rates higher than 500 mV s^{-1} for both reduction peaks. When these two sets of data are fit separately with two lines, two slopes are obtained for each reduction peak. The slope values, 0.46 and 0.58 (Figs. S17d and S18d), indicate that the two reduction peaks both exhibit homogeneous diffusion-controlled properties in low scan rates (60 to 200 mV s^{-1}), while in high scan rates (500 to 1000 mV s^{-1}), the slope values are increased to 0.66 and 0.83 for the two reduction peaks, implying that the diffusion rate of catalyst molecules from the electrode surface lags behind the fast scan rate, possibly due to the electrostatic interaction of positively charged catalyst with the polarized electrode surface. These observations support that **2b** functions as molecular catalyst in a diffusion-controlled regime. In addition, the currents of **2b** grow up apparently with decrease of pH value and the onset potential of catalytic peak is pH dependent (Fig. S19), indicative of a proton coupled reduction process.

Controlled potential electrolysis (CPE) experiments of **2b** in 2.0 M phosphate buffer at pH 7 were conducted in a double-compartment cell using a mercury pool with a 3.1 cm^{-2} superficial area as working electrode. The applied overpotentials were varied from 625 to 850 mV to assess the rate of electrocatalytic hydrogen generation by **2b**. As shows in Fig. 5a, the cumulative charge quantity is negligible at overpotentials below 700 mV, which is consistent with the onset potential of catalytic peak of **2b** in a pH 7 buffer solution. At more negative potentials, the cumulative charge increases almost linearly in the range of overpotentials from 770 to 850 mV (Fig. 5b). After subtracting the charge (0.04 C) required for the two-electron reduction of all molecules of nickel catalyst in the bulk solution from the total consumed charge, the quantity of cumulative charge at an overpotential of 700 mV for 1 min is 0.11 C and it reaches 1.71 C at an overpotential of 825 mV. The corresponding turnover frequency (TOF) is calculated to be 1613 mol H_2 (mol cat)$^{-1}$ h^{-1} cm^{-2}. The TOF values are calculated by using the number of catalyst molecules in the entire bulk solution and therefore provide only lower bounds for the activity of **2b**.

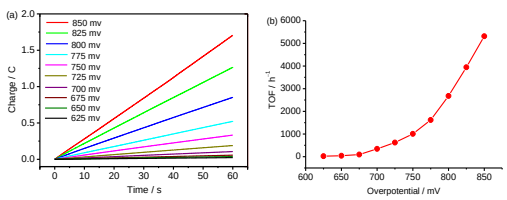

Fig. 5 (a) Charge build-up versus time at various overpotentials over a 1-min interval and (b) turnover frequency versus overpotential for a 5 μM solution of **2b** in 2.0 M phosphate buffer at pH 7.

The extended CPE experiments of 5 μM **2b** were performed in a 2.0 M neutral phosphate buffer at −1.25 V for 60 h to explore the durability of the system. As depicted in Fig. 6, **2b** exhibits an approximately linear increase in the charge accumulation with the extended time of CPE experiments and no considerable loss in activity was observed over 60-h electrolysis. On the basis of consumed charges over 60-h CPE experiments and taking into account the Faradaic efficiency (~91%) for the usage of charge at working electrode (Fig. S20), the TON of H_2 evolution is calculated to be 3.08 × 10^5 mol of H_2 per mol of catalyst, corresponding to an average TOF of 1650 mol H_2 (mol cat)$^{-1}$ h^{-1} cm^{-2}. Similar extended CPE experiments were also made for **1b** and **3b** in neutral aqueous solutions under identical conditions. The TONs of H_2 evolution are 8.20 × 10^4 for **1b** and 1.62 × 10^4 mol of H_2 per mol of catalyst for **3b** over 60-h electrolysis, corresponding to TOFs of 440 and 85 mol H_2 (mol cat)$^{-1}$ h^{-1} cm^{-2} for **1b** and **3b**, respectively. Complex **3b** with an Am3Py2 ligand displays much lower catalytic activity than its analogues **1b** and **2b**, most possibly due to the more negative potential of the catalytic current of **3b** as compared to those of **1b** and **2b**. In comparison, the TON of the literature reported binuclear nickel macrocyclic complex in neutral aqueous solutions is up to 100 TON before the catalyst is totally decomposed during ~1.5-h electrolysis experiment at –1.26 V.[6] The electrocatalytic activity of **2b** is also higher than recently reported efficient non-noble metal-based molecular catalysts of N_x-multidentate ligands measuring under similar conditions but at higher applied potentials, such as $[(PY5Me2)MoO]^{2+}$ (434 mol H_2 (mol cat)$^{-1}$ h^{-1} cm^{-2} at –1.40 V for 71 h),[8] $[(PY5Me2)Co(H_2O)]^{2+}$ (47 mol H_2 (mol cat)$^{-1}$ h^{-1} cm^{-2} at –1.30 V for 60 h),[9] $[(DPA\text{-}Bpy)Co(H_2O)]^{3+}$ (62 mol H_2 (mol cat)$^{-1}$ h^{-1} cm^{-2} at –1.40 V for 1 h),[11] and $[(bztpen)Co(H_2O)]^{2+}$ (860 mol H_2 (mol cat)$^{-1}$ h^{-1} cm^{-2} at −1.25 V for 60 h.[12]

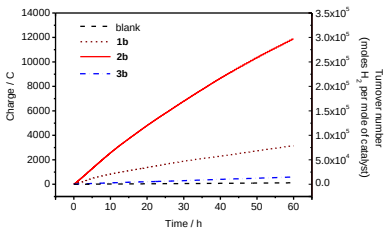

Fig. 6 Charge build-up and turnover number versus time in extended CPE experiments of 5 μM **1b**, **2b**, and **3b** in 2.0 M phosphate buffer at pH 7 and of the blank solution of 2.0 M neutral phosphate buffer at a potential of −1.25 V on a mercury pool electrode; the contribution from the background solution and the charge required for the reduction of all nickel catalyst in the bulk solution have been subtracted from the charge build-up lines of **1b**, **2b**, and **3b**.

The resulting solution following 60-h electrolysis was detected by UV-vis spectroscopy, which showed that the absorptions of **2b** were slowly decreased with extension of electrolysis time (Fig. S21) and the intensity of the band at 260 nm was decreased by about 22% after 60-h CPE experiments. These observations implicate that a slow degradation of the catalyst during long time electrolysis. Furthermore, we made a continuous scan of **2b** in phosphate buffer at pH 7 with a controlled growth mercury drop electrode for 50 cycles between +0.05 to −1.25 V. The catalytic current observably increases during 50-cycle scanning (Fig. S22). After used for 50 cycle scans, the working electrode, washed and reused in a fresh phosphate buffer solution in the absence of catalyst, displayed a CV similar to that of the initial blank CV. This evidence indicates that a small amount of catalyst is weakly adsorbed on the surface of

electrode during multicycle electrolysis, but the adsorbed species readily fall off from the electrode when the applied potential is removed.

In conclusion, mononuclear nickel complexes **1**–**3** with a series of amine-pyridine-based N_5-pentadentate ligands, Am1Py4, Am2Py3, and Am3Py2, were prepared and structurally characterized. The electrochemical studies of **1**−**3** in THF show that the first reduction potential for the Ni^{II}/Ni^{I} couple apparently shifts to positive direction with increase of the number of amine-N atoms in an amine-pyridine-based N_5-pentadentate ligand, while the potential of the second one is less affected. All three nickel complexes can electrochemically catalyze water reduction to produce H_2 in neutral aqueous solutions but with significantly different catalytic activities. Among these nickel complexes, **2b** is the most active electrocatalyst for hydrogen generation from neutral aqueous solutions. The H_2 evolving activity of **2b** in a pH 7 phosphate buffer solution reaches 1650 mol H_2 (mol cat)$^{-1}$ h^{-1} cm^{-2} at −1.25 V, which is more than one-fold higher than that displayed by the analogous cobalt catalyst at the same applied potential and 3–37 fold higher than the activities reported for other nonprecious metal-based molecular catalysts of N_x-multidentate ligands at applied potentials of −1.30 to −1.40 V under otherwise similar measuring conditions.

We are grateful to the Natural Science Foundation of China (Nos. 21373040, 21120102036, 21361130020 and 91233201), the Basic Research Program of China (No. 2014CB239402), the Ph. D. Program Foundation of Ministry of Education of China (No. 20130041110024), the Swedish Research Council, the Swedish Energy Agency and the K & A Wallenberg Foundation for financial support of this work.

Notes and references

[a] State Key Laboratory of Fine Chemicals, DUT-KTH Joint Education and Research Center on Molecular Devices, Dalian University of Technology (DUT), Dalian 116024, China. E-mail: symbueno@dlut.edu.cn

[b] Department of Chemistry, KTH Royal Institute of Technology, Stockholm 10044, Sweden

Electronic supplementary information (ESI) available: Experimental details of preparation and characterization of **1**–**3**, crystal structures and data, as well as CVs. See DOI: 10.1039/c000000x/

1 a) C. Costentin, S. Drouet, M. Robert and J.-M. Saveant, *J. Am. Chem. Soc.*, 2012, **134**, 11235; b) C. Costentin and J.-M. Saveant, *ChemElectroChem*, 2014, **1**, 1226.

2 a) H. I. Karunadasa, E. Montalvo, Y. Sun, M. Majda, J. R. Long and C. J. Chang, *Science*, 2012, **335**, 698; b) V. S. Thoi, Y. Sun, J. R. Long and C. J. Chang, *Chem. Soc. Rev.*, 2013, **42**, 2388.

3 a) V. Artero, M. Chavarot-Kerlidou and M. Fontecave, *Angew.Chem. Int. Ed.*, 2011, **50**, 7238; b) S. Losse, J. G. Vos and S. Rau., *Coord.Chem. Rev.*, 2010, **254**, 2492; c) D. L. DuBois and R. M. Bullock, *Eur. J. Inorg. Chem.*, 2011, **7**, 1017; d) P. Du and R. Eisenberg, *Energy Environ. Sci.*, 2012, **5**, 6012; e) M. Wang, L. Chen and L. Sun, *Energy Environ. Sci.*, 2012, **5**, 6763.

4 A. Begum, G. Moula and S. Sarkar, *Chem.-Eur. J.*, 2010, **16**, 12324.

5 a) B. D. Stubbert, J. C. Peters and H. B. Gray, *J. Am. Chem. Soc.*, 2011,**133**, 18070; b) C. C. McCrory, C. Uyeda and J. C. Peters, *J. Am. Chem. Soc.*, 2012, **134**, 3164; c) F. Quentel, G. Passard and F. Gloaguen, *Energy Environ. Sci.*, 2012, **5**, 7757.

6 J. P. Collin, A. Jouaiti and J. P. Sauvage, *Inorg. Chem.*, 1988, **27**, 1986.

7 P. V. Bernhardt and L. A. Jones, *Inorg. Chem.*, 1999, **38**, 5086.

8 H. I. Karunadasa, C. J. Chang and J. R. Long, *Nature*, 2010, **464**, 1329.

9 Y. Sun, J. P. Bigi, N. A. Piro, M. L. Tang, J. R. Long and C. J. Chang, *J. Am. Chem. Soc.*, 2011, **133**, 9212.

10 Y. Sun, J. Sun, J. R. Long, P. Yang and C. J. Chang, *Chem. Sci.*, 2013, **4**, 118.

11 W. M. Singh, T. Baine, S. Kudo, S. Tian, X. A. Ma, H. Zhou, N. J. DeYonker, T. C. Pham, J. C. Bollinger, D. L. Baker, B. Yan, C. E. Webster and X. Zhao, *Angew. Chem. Int. Ed.*, 2012, **51**, 5941.

12 P. Zhang, M. Wang, F. Gloaguen, L. Chen, F. Quentel and L. Sun, *Chem. Commun.*, 2013, **49**, 9455.

13 L. Chen, M. Wang, K. Han, P. Zhang, F. Gloaguen and L. Sun, *Energy Environ. Sci.*, 2014, **7**, 329.

14 a) S. Trasatti, *J. Electroanal.Chem.*, 1972, **39**, 163; b) M. H. Miles, *J. Electroanal. Chem.*, 1975, **60**, 89.

15 a) O. Pantani, E. Anxolabehere-Mallart, A. Aukauloo and P. Millet, *Electrochem.Commun.*, 2007, **9**, 54; b) P.-A. Jacques, V. Artero, J. Pecaut and M. Fontecave, *Proc. Natl. Acad. Sci. U. S. A.*, 2009, **106**, 20627.

16 O. R. Luca, S. J. Konezny, J. D. Blakemore, D. M. Colosi, S. Saha, G. W. Brudvig, V. S. Batista and R. H. Crabtree, *New-J. Chem.*, 2012, **36**, 1149.

17 a) W. Zhang, J. Hong, J. Zheng, Z. Huang, J. Zhou and R. Xu, *J. Am. Chem. Soc.*, 2011, **133**, 20680; b) J. Han, W. Zhang, T. Zhou, X. Wang and R. Xu, *RSC Adv.*, 2012, **2**, 8293; c) Z. Han, L. Shen, W. W. Brennessel, P. L. Holland and R. Eisenberg, *J. Am. Chem. Soc.*, 2013, **135**, 14659.

18 a) M. L. Helm, M. P. Stewart, R. M. Bullock, M. R. DuBois and D. L. DuBois, *Science*, 2011, **333**, 863; b) D. H. Pool, M. P. Stewart, M. O'Hagan, W. J. Shaw, J. A. S. Roberts, R. M. Bullock and D. L. DuBois, *Proc. Natl. Acad. Sci. U. S. A.*, 2012, **109**, 15634; c) S. Wiese, U. J. Kilgore, M.-H. Ho, S. Raugei, D. L. DuBois, R. M. Bullock and M. L. Helm, *ACS Catal.*, 2013, **3**, 2527.

19 M. S. Vad, A. Nielsen, A. Lennartson, A. D. Bond, J. E. McGrady and C. J. McKenzie, *Dalton Trans.*, 2011, **40**, 10698.

20 N. Ortega-Villar, V. M. Ugalde-Saldivar, M. C. Munoz, L. A. Ortiz-Frade, J. G. Alvarado-Rodriguez, J. A. Real and R. Moreno-Esparza, *Inorg. Chem.*, 2007, **46**, 7285.

21 A. J. Bard and L. R. Faulkner, *Electrochemical Methods: Fundamentals and Applications, 2nd ed.*, Wiley: New York, 2001.

